

Article

An Impact-Based Frequency Up-Converting Hybrid Vibration Energy Harvester for Low Frequency Application

Zhenlong Xu ^{1,*} , Wen Wang ¹ , Jin Xie ², Zhonggui Xu ², Maoying Zhou ¹ and Hong Yang ³

¹ School of Mechanical Engineering, Hangzhou Dianzi University, Hangzhou 310018, China; wangwn@hdu.edu.cn (W.W.); myzhou@hdu.edu.cn (M.Z.)

² State Key Laboratory of Fluid Power and Mechatronic Systems, Zhejiang University, Hangzhou 310027, China; xiejin@zju.edu.cn (J.X.); xuzhonggui@zju.edu.cn (Z.X.)

³ School of Medicine, Zhejiang University, Hangzhou 310058, China; yanghong86@zju.edu.cn

* Correspondence: xzl@hdu.edu.cn; Tel.: +86-571-8691-9155

Received: 23 September 2017; Accepted: 31 October 2017; Published: 2 November 2017

Abstract: In this paper, a novel impact-based frequency up-converting hybrid energy harvester (FUCHEH) was proposed. It consisted of a piezoelectric cantilever beam and a driving beam with a magnetic tip mass. A solenoid coil was attached at the end of the piezoelectric beam. This innovative configuration amplified the relative motion velocity between magnet and coil, resulting in an enhancement of the induced electromotive force in the coil. An electromechanical coupling model was developed and a numerical simulation was performed to study the principle of impact-based frequency up-converting. A prototype was fabricated and experimentally tested. The time-domain and frequency-domain analyses were performed. Fast Fourier transform (FFT) analysis verified that fundamental frequencies and coupled vibration frequency contributes most of the output voltage. The measured maximum output power was 769.13 μW at a frequency of 13 Hz and an acceleration amplitude of 1 m/s^2 , which was 3249.4%- and 100.6%-times larger than that of the frequency up-converting piezoelectric energy harvesters (FUCPEH) and frequency up-converting electromagnetic energy harvester (FUCEMEH), respectively. The root mean square (RMS) voltage of the piezoelectric energy harvester subsystem (0.919 V) was more than 16 times of that of the stand-alone PEH (0.055 V). This paper provided a new scheme to improve generating performance of the vibration energy harvester with high resonant frequency working in the low-frequency vibration environment.

Keywords: mechanical impact; frequency up-converting; hybrid energy harvester; piezoelectric; electromagnetic

1. Introduction

With the development of the technology, the embedded wireless sensors and portable microelectronics devices are widely used in industry, agriculture, medicine, and so on. Energy supply is a critical challenge during the practical applications. Capturing the ambient energy, known as energy harvesting provides a clean, renewable, and uninterrupted solution to power the low power-consuming devices. The common energy sources in the ambient environment include solar, wind, thermal, vibration, and radiation energy. Among them, the vibration energy is widely distributed, and possesses high energy density. Generally, the transduction mechanisms of vibration energy harvesting can be divided into piezoelectric [1], electromagnetic [2], electrostatic [3], and magnetoelectric [4]. Due to the high electromechanical coupling coefficients, simple processing, and no external power supply, piezoelectric energy harvesting is the one of the most reported transduction mechanism. As the power

supply of the implantable and portable microelectronic devices, compact size is the demand for the energy harvesters. However, most of the micro-level piezoelectric energy harvesters (PEHs) operate at resonant frequency of 100 Hz or higher [5–7]. As a result, resonant vibration energy harvesters suffer from dramatically reduced output power in the low frequency range (less than 30 Hz). In recent years, a great deal of research has been done to improve the generating performance and enhance the environmental adaptability of the PEHs in a low-frequency environment.

Mechanical frequency up-conversion technology was one typical approach proposed for the low frequency application, in which the low-frequency ambient vibration can be converted to the high-frequency vibration of micro energy harvester. Umeda et al. [8] firstly applied the impact of a steel ball on the piezoelectric membrane for frequency up-converting energy harvesting. Two-stage energy harvesting concept was proposed by Rastegar et al. [9]. As the first stage, low-frequency oscillation system intermittently transfers the mechanical energy to the secondary stage system with significantly higher natural frequency by interaction contact. Then, the secondary system converts the mechanical energy to electric energy. After the contact, the generating element vibrates with its own high resonant frequency. As a result, the mechanical frequency is up-converted. Based on this concept, related research on frequency up-converting piezoelectric energy harvester (FUCPEH) has been widely conducted. The interaction contact can be further divided into two types. One is mechanical impact [10–12], and the other is mechanical plucking [13–16]. In the above-mentioned designs, the low-frequency oscillator is only used to trigger the high frequency vibration of the generating element. The kinetic energy of the driving element is only harvested by the generating element. Liu et al. [17] replaced the driving element with a low-frequency piezoelectric beam, which not only generates electric power, but also introduce high frequency oscillation of the other piezoelectric generating beam. Vijayan et al. [18] studied the dynamic characteristics of two coupled impacting piezoelectric beams. It was demonstrated that the power generated by the coupled system is sensitive to the thickness ratio of the beams and the clearance. Edwards et al. [19] collected the kinetic energy of the driving beam by the electromagnetic induction and presented a frequency up-converting hybrid energy harvester (FUCHEH).

In the literature mentioned above, most of theoretical models ignored the influence of the electromechanical coupling term on the equivalent stiffness of the system. The electrical damping induced by the load resistance was considered to be constant and independent of the excitation frequency. Certainly, an accurate theoretical model of the frequency up-converting vibration energy harvester is required for optimization design. In addition, the time-domain responses were analyzed generally, whereas the frequency-domain analysis has almost never been reported. As a result, the contribution of excitation frequencies to the output power is not clear.

In this paper, we report an impact-based FUCHEH, using piezoelectric and electromagnetic conversion mechanisms. The electromechanical coupling model is established in Sections 2 and 3 simulates and analyzes the displacement, velocity, and open-circuit voltages responses of piezoelectric and magnetic oscillators. Section 4 presents the prototype and an experimental testing system. The generating characteristics of the FUCHEH are measured and discussed.

2. Design and Modeling

2.1. Design and Working Principle

Figure 1 illustrates the schematic diagram of the proposed frequency up-converting hybrid energy harvester. It consists of a bimorph piezoelectric cantilever beam with a high resonant frequency and a cantilevered driving beam with low resonant frequency. A cylindrical permanent magnet is placed at the end of the driving beam as a proof mass. A solenoid coil is attached at the end of the piezoelectric beam. The axis of the magnet is configured to be coaxially aligned with the coil. The innovation of this FUCHEH is the arrangement of the magnet and coil. This innovative configuration amplifies the relative motion velocity between the magnet and coil, resulting in an enhancement of the induced

electromotive force in the coil. When the FUCHEH is subjected to the ambient excitation, electricity is generated in the piezoelectric beam based on the piezoelectric effect. Meanwhile, an electromotive force is induced in the coil due to the electromagnetic induction.

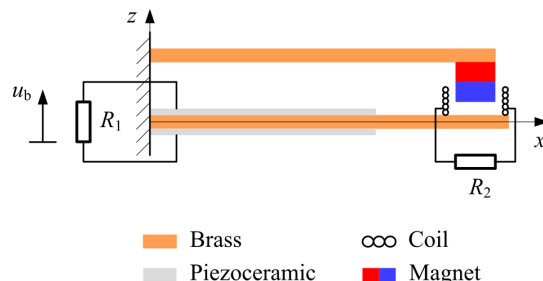


Figure 1. Schematic diagram of the proposed frequency up-converting hybrid energy harvester (FUCHEH).

When a low-frequency external excitation near the resonance of the magnetic oscillator is applied on the FUCHEH, the magnetic oscillator vibrates downward and impacts the piezoelectric beam. This impact can be regarded as an inelastic collision [10]. However, the collision time is so short that the velocities of two oscillators are presumed to be redefined instantaneously. Accordingly, part of the kinetic energy of the magnetic oscillator is converted to potential energy of the piezoelectric beam. After the contact, two oscillators vibrate independently until the collision of the next cycle. Especially, the piezoelectric oscillator vibrates with its own high resonant frequency. As a result, the mechanical frequency is up-converted. Additionally, the piezoelectric beam works as a mechanical stopper for the magnetic oscillator, which is similar to the mechanism of widening bandwidth by impact. Consequently, a broadband frequency response during frequency sweep can be realized.

2.2. Theoretical Modeling

Under the low-level and low-frequency excitation, the deflection of piezoelectric beam satisfies the linear deformation. Although the magnetic oscillator can vibrate with large amplitude at resonance, the piezoelectric beam constrains its large deformation just like a flexible stopper. Therefore, its geometry nonlinearity is neglected. In a word, the FUCHEH can be reduced to a piecewise linear dynamic system. In addition, the rotation inertia of the magnetic proof mass and the induction coil are neglected. Both cantilever beams are considered to be Euler-Bernoulli beams. The lumped parameter model, known as spring-mass-damping model, is presented to illustrate the dynamic response of the impact-based FUCHEH, as shown in Figure 2. Piezoelectric beam and magnetic oscillator are simplified as spring-mass-damping oscillators with the equivalent mass, M_1 and M_2 , spring stiffness, K_1 and K_2 , and damping, C_1 and C_2 , respectively. The external load resistances connected to piezoceramic patches and induction coil are R_1 and R_2 , respectively. Two piezoceramic patches are connected in series. d is the separation distance between two oscillators in the vertical direction at static condition. The electromechanical coupling coefficients for the piezoelectric and electromagnetic transduction mechanisms are assumed to be θ_p and θ_e , respectively. The calculation models of θ_p and θ_e have been reported previously [20,21]. u_b is the displacement of the base. Assume that the displacements of piezoelectric and magnetic oscillators relative to base are r_1 and r_2 , respectively. Figure 3 presents the equivalent circuits of the piezoelectric energy harvester (PEH) subsystem and the electromagnetic energy harvester (EMEH) subsystem, respectively. It is worth noting that the interaction between piezoelectric and magnetic oscillators consists of not only the impact force, but also the electromagnetic damping force induced by the electromagnetic induction. This is an important distinction from the previously reported configurations.

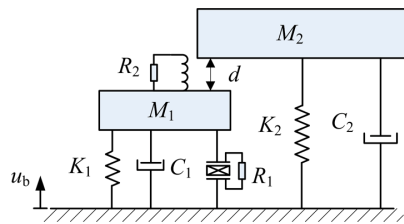


Figure 2. Lumped parameter model of the FUCHEH.

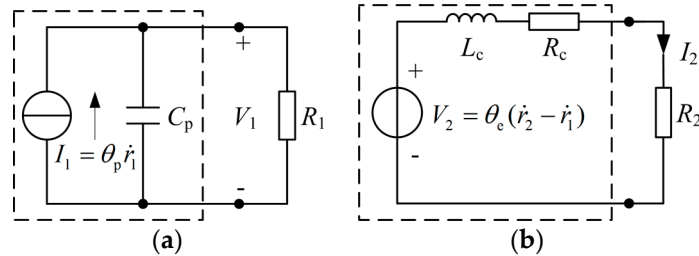


Figure 3. Equivalent circuits. (a) The piezoelectric energy harvester (PEH) subsystem; (b) The electromagnetic energy harvester (EMEH) subsystem.

When the separation distance, d , is greater than zero, two oscillators are not in contact and vibrate independently. As reported by Tang and Yang [22], the non-impact electromechanical coupling equations for piezoelectric oscillator are given by Equations (1) and (2), while Equations (3) and (4) for magnetic oscillator.

$$M_1 \ddot{r}_1 + C_1 \dot{r}_1 + K_1 r_1 - \theta_p V_1 - \theta_e I_2 = -\mu_1 M_1 \ddot{u}_b \quad (1)$$

$$\theta_p \dot{r}_1 + C_p \dot{V}_1 + V_1 / R_1 = 0 \quad (2)$$

$$M_2 \ddot{r}_2 + C_2 \dot{r}_2 + K_2 r_2 + \theta_e I_2 = -\mu_2 M_2 \ddot{u}_b \quad (3)$$

$$-\theta_e (\dot{r}_2 - \dot{r}_1) + (R_c + R_2) I_2 = 0 \quad (4)$$

where μ_1 and μ_2 are the correction factors of forcing function. C_p is the clamped capacitance of the piezoelectric beam. V_1 is the voltage across load R_1 . I_2 is the induced current in the coil. The coil inductance is neglected due to the low-frequency excitation [23]. Noting that, in these equations, the effects of coupling terms on the equivalent spring stiffness and damping are taken into account.

When the separation distance reduces to zero, the magnetic oscillator impacts the piezoelectric beam. In order to effectively describe the complex dissipation mechanisms during the collision, the coefficient of restitution e is defined. The velocities of piezoelectric and magnetic oscillators at the moment after collision are respectively given by

$$v_{11} = [(M_1 v_{10} + M_2 v_{20}) - e M_2 (v_{10} - v_{20})] / (M_1 + M_2) \quad (5)$$

$$v_{21} = [(M_1 v_{10} + M_2 v_{20}) + e M_1 (v_{10} - v_{20})] / (M_1 + M_2) \quad (6)$$

where v_{10} and v_{20} are the instantaneous velocities of the piezoelectric and magnetic oscillators before collision, respectively. Then, two oscillators will separate and vibrate independently until they collide during the next cycle.

According to the previously described equations, the instantaneous output power generated by the PEH and the EMEH elements can be, respectively, written as

$$P_p = V_1^2 / R_1 \quad (7)$$

$$P_e = I_2^2 R_2 \quad (8)$$

As a result, the total instantaneous power extracted from the FUCHEH is the sum of P_p and P_e .

3. Numerical Simulation

Based on the theoretical model of the FUCHEH, numerical simulation was performed to research the displacement, velocity, and voltage responses by using the ordinary differential equation solver ode45 in MATLAB® (R2012b, MathWorks Inc.: Natick, MA, USA). For the sake of distinction, the substrate of piezoelectric beam was labeled as substrate A, while that of the magnetic oscillator was substrate B. Both mechanical damping ratios of PEH and EMEH parts were set to 0.02. The initial separation distance at static state was set to 2.4 mm. A harmonic excitation was applied to the FUCHEH with the acceleration amplitude of 1 m/s². The geometric and material parameters are given in Table 1, based on the prototype fabricated.

Table 1. Geometric and material parameters of the FUCHEH.

| Parameter | Value |
|--|------------------|
| Substrate A length × width × thickness (mm ³) | 80 × 20 × 0.53 |
| Substrate B length × width × thickness (mm ³) | 80 × 20 × 0.53 |
| Substrate density (kg/m ³) | 8920 |
| Young's modulus of substrate A (GPa) | 80 |
| Young's modulus of substrate B (GPa) | 110 |
| Piezoceramic length × width × thickness (mm ³) | 40 × 20 × 0.2 |
| Piezoceramic density (kg/m ³) | 7386 |
| Young's modulus of piezoceramic (GPa) | 60.6 |
| Piezoelectric stress constant (C/m ²) | -16.6 |
| Dielectric permittivity (nF/m) | 25.55 |
| Coefficient of restitution | 0.7 |
| Magnet radius × height (mm ²) | 10 × 10 |
| Residual magnetic flux density (T) | 1.3 |
| Magnet density (kg/m ³) | 7500 |
| Coil turns | 2000 |
| Coil inner radius × outer radius × height (mm ³) | 12.5 × 14.2 × 20 |
| Coil resistance (Ω) | 362 |

Figure 4 shows the simulated time-domain responses of the piezoelectric and magnetic oscillators that are driven by base excitation. The trends were identical to what we described before. Both load resistances connected to piezoceramic patches and induction coil are assumed to be 10⁹ Ω. As a result, the numerical simulation is considered to be conducted under the open-circuit condition. The theoretical natural frequencies of the piezoelectric and magnetic oscillators are about 42.3 Hz and 12.6 Hz, respectively. Therefore, the excitation frequency is set to 12.6 Hz. In Figure 4a, it can be seen that the displacement of the magnetic oscillator is similar to the sinusoidal curve. The amplitude slightly changes during the oscillation. However, the displacement of the piezoelectric oscillator abruptly rises as the collision occurs. At this moment, two oscillators get in contact with each other and part of the kinetic energy harvested by the magnetic oscillator is transferred to the piezoelectric oscillator through impact, resulting in a rise of its displacement. Meanwhile, the velocities of two oscillators are discontinuous and are assigned new values. After the separation, the piezoelectric oscillator vibrates independently at high frequency and its displacement gradually decays until the next impact occurs. So far, the low-frequency excitation is up-converted.

Concomitantly, there are discrete spikes in the open-circuit voltage waveform generated from the PEH element (V_1) when collision occurs and then exponential decay, as shown in Figure 4b. Obviously, they are triggered by the impact, which is coinciding with the displacement response. The decay rate is not only determined by the mechanical damping, but also the electromagnetic damping. There is

also a sudden change for the induced voltage V_2 in the coil as impacting. It jumps from negative value to positive one abruptly. After the collision, its trajectory is similar to the sinusoidal curve.

Figure 5a,b show the phase portraits of the piezoelectric and magnetic oscillators, respectively. Obviously, each collision is accompanied by a velocity jump up for the piezoelectric oscillator and a velocity jump down for the magnetic oscillator. After the impact, the piezoelectric oscillator experiences attenuations of displacement and velocity until the moment that the next collision occurs. There is no obvious change for the phase trajectory of magnetic oscillator, which is due to the large initial separation distance between two oscillators.

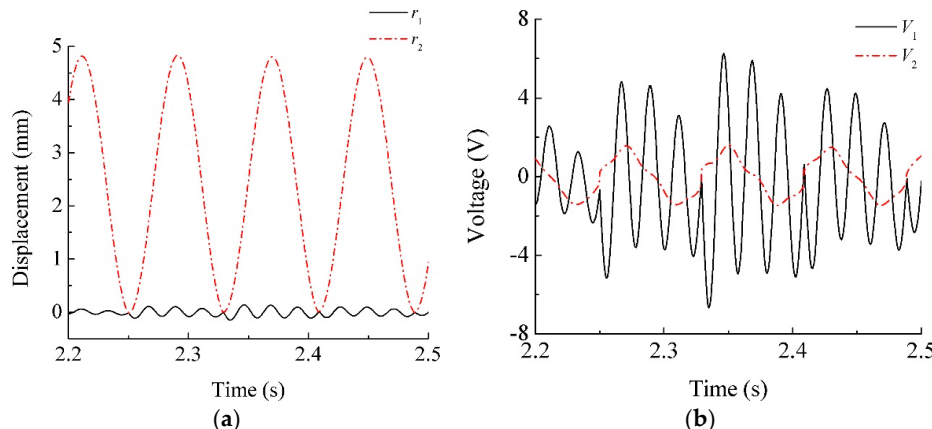


Figure 4. The simulated time-domain responses of the piezoelectric and magnetic oscillators. (a) Relative tip displacements to the base; (b) Open-circuit voltages.

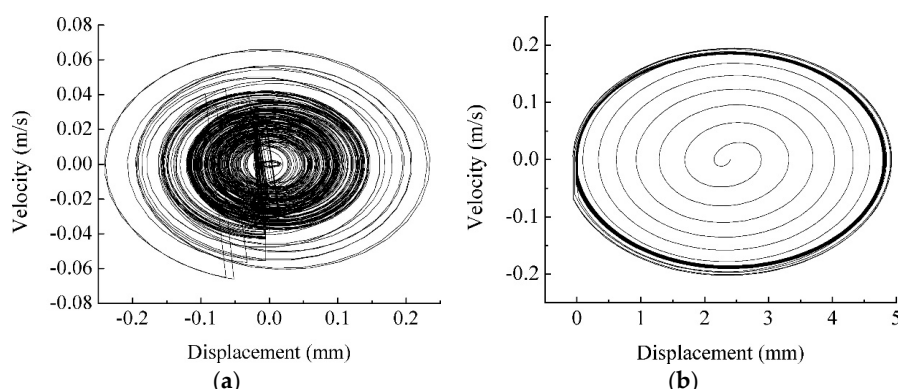


Figure 5. Phase portraits. (a) The piezoelectric oscillator; (b) The magnetic oscillator.

4. Experiment and Discussion

In order to validate the feasibility of the FUCHEH, a meso-scale prototype was fabricated, as shown in Figure 6a. It consists of a bimorph piezoelectric cantilever beam, a cantilevered driving beam with magnetic proof mass (NdFeB N35), and an induction coil. The substrate A and substrate B are, respectively, made of brass and phosphor bronze. The piezoceramic is lead zirconate titanate (PZT-5H). The geometric and material parameters are summarized in Table 1. The FUCHEH prototype is clamped to an electromagnetic shaker (LDS V406). The excitation signal is generated by the vibration controller (Spider 81B) and amplified by a power amplifier (LDS PA100E). The excitation acceleration is measured by an accelerometer (PCB 352C33), and is then controlled and monitored by the vibration controller. Finally, all of the voltages that are generated from PEH and EMEH subsystems are input into the vibration controller and recorded. Figure 6b shows the experimental system for the FUCHEH.

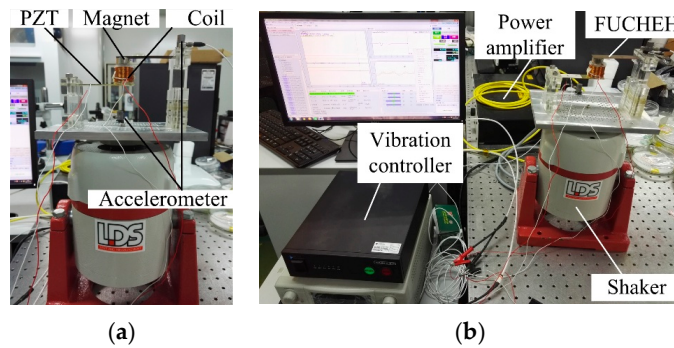


Figure 6. (a) Prototype of the FUCHEH; (b) Experimental system for the FUCHEH.

The measured resonant frequencies of piezoelectric and magnetic oscillators, respectively, were 40.5 Hz and 12.8 Hz, which are close to the theoretical value. Therefore, the excitation frequency was set to 13 Hz, so as to capture maximum low-frequency vibration energy. A harmonic excitation acceleration was applied to the FUCHEH with the amplitude of 1 m/s^2 . The separation distance was set to 2.4 mm. By using the logarithmic decrement method, the mechanical damping ratios of piezoelectric and magnetic oscillators are measured to be 0.02 and 0.015, respectively.

Figure 7 shows the measured open-circuit voltages from PEH and EMEH elements, and a comparison with the theoretical results. It is clear that the experimental results have the similar waveforms as that of the theoretical results. The voltage waveform generated from EMEH seems to be quasi-periodic signal with a root mean square (RMS) value of 1.05 V. This voltage, V_2 , jumps from negative value to positive one instantaneously when two oscillators collide. This phenomenon is the same as what described in simulation result, as shown in Figure 7b. The subscripts "t" and "e" stand for theoretical and experimental results, respectively. However, there are multiple spikes in voltage V_1 during the collision, which are not displayed in the simulation results. According to the V_1 waveform and value of V_2 , we can conclude that there are sub-impacts after the first impact [24]. After the first impact, the piezoelectric beam absorbs some kinetic energy and vibrates in the same direction as that of the magnetic oscillator. Due to the higher fundamental frequency, it reverses its trajectory, catches up with the magnet again, and generates the sub-impacts. The RMS value of V_1 is 4.20 V. Note that some kinetic energy is dissipated in each inelastic collision. Sub-impact will reduce the energy conversion efficiency of the FUCHEH. Accordingly, it is necessary to explore the occurrence condition of the sub-impact and its influence on the output power, in order to optimize the generating performance of the FUCHEH. However, the related research is not the focus of this paper, which will be performed in the future.

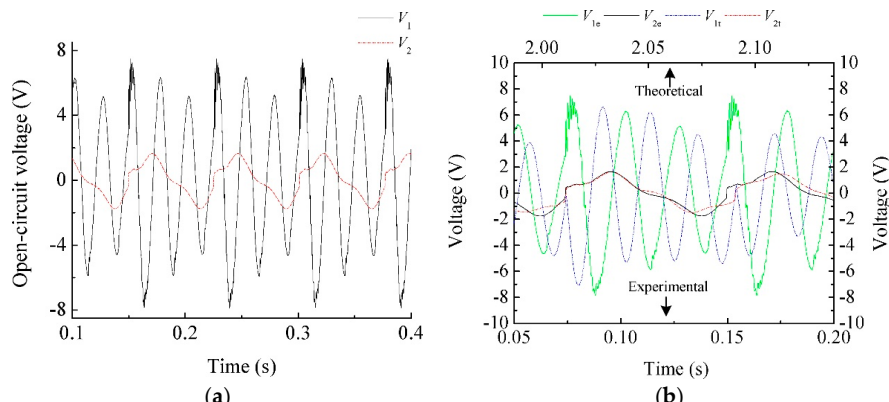


Figure 7. (a) The measured open-circuit voltages from the PEH and EMEH subsystems, and (b) Comparison between theoretical and experimental open-circuit voltage waveforms.

Frequency domain analysis of the time-domain signal can be carried out by using the fast Fourier transform (FFT). Figure 8 shows the FFT of open-circuit voltage corresponding to Figure 7a. From Figure 8a, there are five frequency components for the piezoelectric oscillator. They are 13.3 Hz, 26.3 Hz, 39.6 Hz, 52.9 Hz, and 79.2 Hz. There is no doubt that 13.3 Hz and 39.6 Hz corresponds to the fundamental frequencies of magnetic and piezoelectric oscillators, respectively. 26.3 Hz is close to the value $\sqrt{(K_1 + K_2)/(M_1 + M_2)/(2\pi)}$. That is to say, two oscillators undergo the coupled vibration for a short time after the collision. 52.9 Hz and 79.2 Hz stand for the double frequency components of coupled vibration frequency and fundamental frequency, respectively. In Figure 8b, only the first three frequencies occupy large weight, i.e., 13.3 Hz, 26.3 Hz, and 39.6 Hz. In a word, impact induces multiple frequency components, resulting in complex dynamic behaviors. It is indicated that the fundamental frequency and the coupled vibration frequency contributes most output voltage for the PEH and EMEH subsystems. Furthermore, sub-impact is mainly affected by the fundamental frequencies of oscillators and coupled vibration frequency.

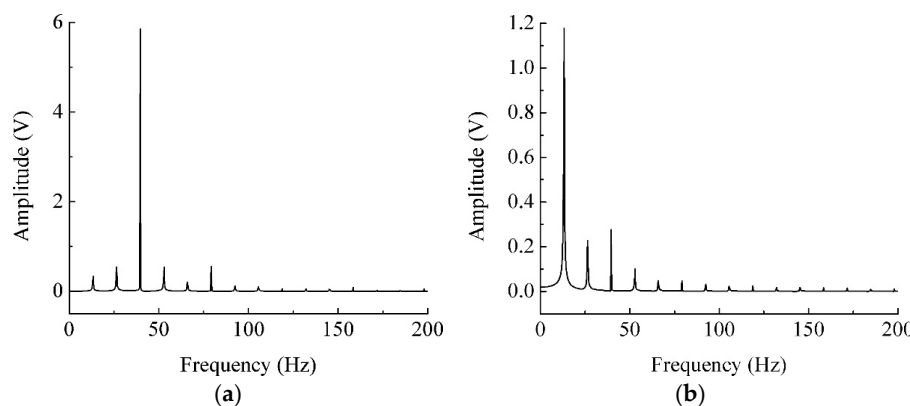


Figure 8. Fast Fourier transform (FFT) of open-circuit voltage. (a) V_1 ; (b) V_2 .

In order to output the maximum power, the load resistances connected are optimized by experimental tests. Based on the conclusion reported previously [21], the load resistances R_1 was optimized firstly. Figure 9a plots the output power of the FUCHEH delivered to different load resistances R_1 for the PEH part. The coil was set to be open-circuit. When the resistance equaled $40 \text{ k}\Omega$, the power reached the maximum. After that, the matched R_1 was connected to piezoceramic layers and were kept constant. The load resistance connected to the induction coil, R_2 was optimized and the matched value was 400Ω , as shown in Figure 9b.

Figure 10 shows the comparison between experimental and theoretical output power frequency responses for the FUCHEH. The matched R_1 and R_2 are connected. The average output power from the PEH (P_1) and EMEH (P_2) subsystems vary with the changing of excitation frequency. It can be seen that the experimental results show the similar trend as that of the theoretical ones. They also agree well with each other at the first resonance. At the second resonance, the noticeable disparity is due to the varying of mechanical damping at higher vibration frequencies. Note that the theoretical values of mechanical damping ratios are presumed to be constant. In this paper, the performance at the first resonance is the focus of attention. The measured P_1 reaches the maximum $21.11 \mu\text{W}$ at 13 Hz. That is to say, the generating performance of the FUCHEH in the low-frequency range depends on the vibration of the driving oscillator. The measured maximum output power of P_1 is 2.8% of that from the EMEH subsystem ($748.02 \mu\text{W}$). The reasons for such a large difference in output power can be summarized as two aspects: (1) the electromagnetic damping force consumes some kinetic energy of the magnetic oscillator, resulting in the decrease of kinetic energy transferred to the PEH subsystem through collision. Moreover, the deformation of the piezoelectric patch is small, due to the small size and large stiffness. Consequently, the PEH subsystem generated limited electric power; (2) the

capacitive reactance of the PEH subsystem is much larger than the optimized load resistance R_1 under the condition of low vibration frequency, which divided large portion of the output voltage. However, when the scale of the FUCHEH is reduced to micro-scale, this difference will be narrowed. That is because the size reduction of the magnet and induction coil will sacrifice generating performance of the EMEH subsystem.

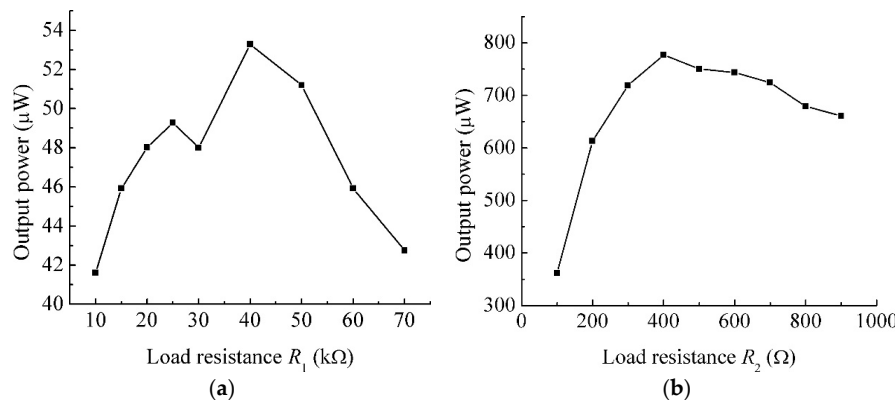


Figure 9. Output power of the FUCHEH with different load resistances. **(a)** The coil is open-circuit and R_1 varies; **(b)** The matched R_1 is connected to the piezoceramic patches and R_2 varies.

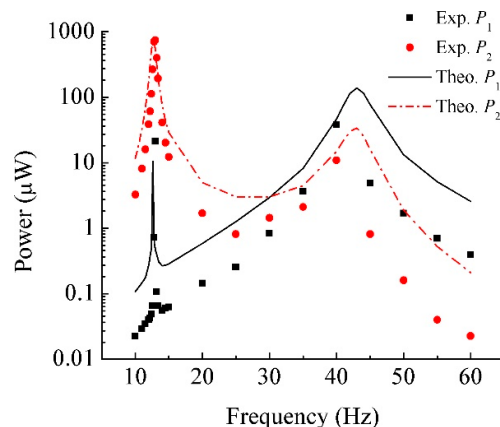


Figure 10. Comparison between experimental and theoretical output power frequency responses for the FUCHEH.

The sweep spectrum analysis was performed in order to search for the resonant frequencies of the FUCHEH, as illustrated in Figure 11. The excitation frequency was swept from 10 Hz to 60 Hz with the sweep rate 0.5 Hz/s. It is shown that the resonant frequencies locate at 13.5 Hz and 40 Hz, respectively. That is to say, the first resonant frequency shifts to the right, while the second one shifts to the left. The right shift conforms the characteristic of hardening spring, which is induced by the collision between piezoelectric and magnetic oscillators. They act as a flexible stopper for each other. The left shift demonstrates the inherent piezoelectric nonlinearity of PZT-5H [25].

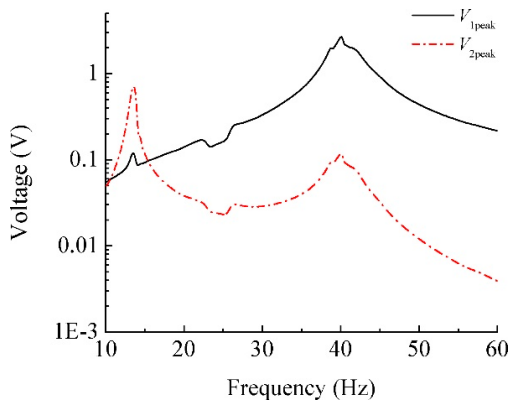


Figure 11. Sweep spectrum analysis for the output voltage frequency responses of the FUCHEH.

If the substrate B and magnet are removed, the stand-alone PEH is developed, which suffers no effect of impact. Similarly, a frequency up-converting piezoelectric energy harvester (FUCPEH) can be produced when the inductance coil of the FUCHEH is open-circuit. A frequency up-converting electromagnetic energy harvester (FUCEMEH) can be formed when the piezoelectric patches of the FUCHEH are short-circuit. Figure 12a illustrates the comparison of output voltages from the PEH subsystem, FUCPEH, and stand-alone PEH. The matched R_1 and R_2 are connected. The excitation frequency is 13 Hz. The RMS voltage of the PEH subsystem is 0.919 V, which is 94.5% of that of the FUCPEH (0.973 V) and more than 16 times of that of the stand-alone PEH (0.055 V). Accordingly, the impact-based frequency-up converting mechanism significantly improves the generating performance of PEH in the low frequency environment. Because part of kinetic energy is harvested through the electromagnetic induction, the RMS voltage generated from the FUCHEH is less than that from the FUCPEH. The comparison of output voltages from the EMEH subsystem and FUCEMEH is presented in Figure 12b. Their RMS values are 0.547 V and 0.553 V. Although the RMS voltages from the subsystems of the FUCHEH are less than that from the frequency up-converting energy harvester with one transduction mechanism, the overall output power of the FUCHEH is 769.13 μ W, which is 3249.4%- and 100.6%-times larger than that of the FUCPEH and FUCEMEH, respectively. Consequently, the FUCHEH proposed contributes to improving the generating performance of the conventional FUCPEH in the low-frequency vibration environment.

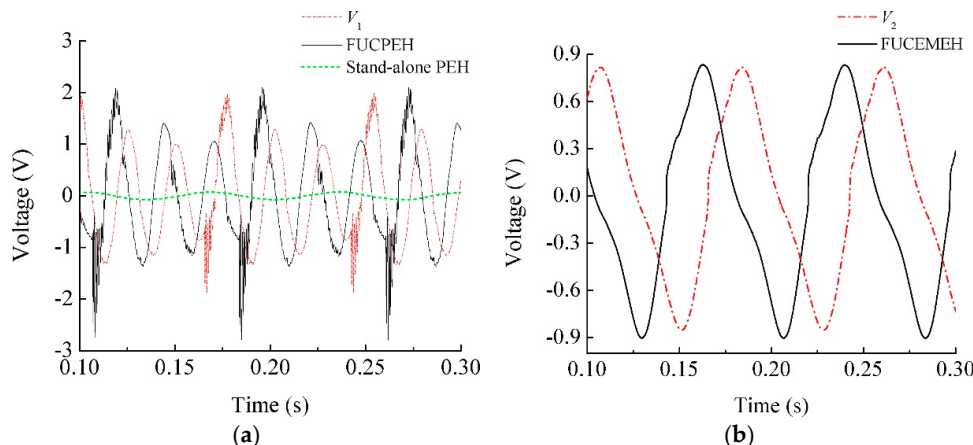


Figure 12. Comparison of output voltages at 13 Hz and 1 m/s^2 . (a) Voltages from the PEH subsystem, FUCPEH and stand-alone PEH; (b) Voltages from the EMEH subsystem and FUCEMEH.

5. Conclusions

In this paper, a novel impact-based frequency up-converting hybrid energy harvester combining piezoelectric and electromagnetic transduction mechanisms was proposed. The electromechanical coupling equations were derived with consideration of the effects of electromechanical coupling terms. The displacements, output voltages, and phase portraits for the piezoelectric and magnetic oscillators were numerically simulated under the open-circuit condition, so as to observe the principle of impact-based frequency up-converting. A prototype was fabricated and experimentally tested. The measured results agreed well with the theoretical results in the low-frequency range. The phenomenon of sub-impact was observed, which should be avoided in order to enhance the amount of harvested kinetic energy. FFT analysis verified that fundamental frequencies and coupled vibration frequency contributes most of the output voltage. The connected load resistances were optimized to maximize the output power of the FUCHEH. The measured maximum output power was 769.13 μ W at frequency of 13 Hz and acceleration amplitude of 1 m/s², which is 3249.4%- and 100.6%-times larger than that of the FUCPEH and FUCEMEH, respectively. The RMS voltage of the PEH subsystem (0.919 V) is more than 16 times of that of the stand-alone PEH (0.055 V). The sweep spectrum analysis showed the effect of hardening spring induced by the collision and the effect of the inherent piezoelectric nonlinearity of PZT-5H. The experimental results validated the feasibility of the FUCHEH, which provided a new scheme to improve generating performance of the vibration energy harvester with high resonant frequency working in the low-frequency vibration environment. Our future work will focus on optimizing the generating performance of this device.

Acknowledgments: This work was supported in part by Zhejiang Provincial Natural Science Foundation of China (Grant No. LZ16E050001) and in part by the National Natural Science Foundation of China (Grant No. 51275465, No. 51465027).

Author Contributions: Zhenlong Xu conceived of the work, developed the theoretical model, and designed the experiments. Zhenlong Xu and Zhonggui Xu set up and conducted the experiments. Hong Yang edited the English language. All authors contributed to analyzing the experimental data and writing the paper.

Conflicts of Interest: The authors declare no conflict of interest.

References

1. Abdelkefi, A.; Barsallo, N.; Tang, L.; Yang, Y.; Hajj, M.R. Modeling, validation, and performance of low-frequency piezoelectric energy harvesters. *J. Intell. Mater. Syst. Struct.* **2013**, *25*, 1429–1444. [[CrossRef](#)]
2. Tao, K.; Wu, J.; Tang, L.; Xia, X.; Lye, S.W.; Miao, J.; Hu, X. A novel two-degree-of-freedom MEMS electromagnetic vibration energy harvester. *J. Micromech. Microeng.* **2016**, *26*, 035020. [[CrossRef](#)]
3. Mitcheson, P.D.; Green, T.C. Maximum Effectiveness of Electrostatic Energy Harvesters when Coupled to Interface Circuits. *IEEE Trans. Circuits Syst. I* **2012**, *59*, 3098–3111. [[CrossRef](#)]
4. Li, P.; Wen, Y.; Jia, C.; Li, X. A Magnetolectric Composite Energy Harvester and Power Management Circuit. *IEEE Trans. Ind. Electron.* **2011**, *58*, 2944–2951. [[CrossRef](#)]
5. Elfrink, R.; Kamel, T.M.; Goedbloed, M.; Matova, S.; Hohlfeld, D.; van Andel, Y.; van Schaijk, R. Vibration energy harvesting with aluminum nitride-based piezoelectric devices. *J. Micromech. Microeng.* **2009**, *19*, 094005. [[CrossRef](#)]
6. Shen, D.; Park, J.-H.; Noh, J.H.; Choe, S.-Y.; Kim, S.-H.; Wikle, H.C.; Kim, D.-J. Micromachined PZT cantilever based on SOI structure for low frequency vibration energy harvesting. *Sens. Actuators A Phys.* **2009**, *154*, 103–108. [[CrossRef](#)]
7. Kim, M.; Hwang, B.; Ham, Y.-H.; Jeong, J.; Min, N.K.; Kwon, K.-H. Design, fabrication, and experimental demonstration of a piezoelectric cantilever for a low resonant frequency microelectromechanical system vibration energy harvester. *J. Micro-Nanolithogr. MEMS MOEMS* **2012**, *11*, 033009. [[CrossRef](#)]
8. Umeda, M.; Nakamura, K.; Ueha, S. Analysis of the Transformation of Mechanical Impact Energy to Electric Energy Using Piezoelectric Vibrator. *Jpn. J. Appl. Phys.* **1996**, *35*, 3267–3273. [[CrossRef](#)]

9. Rastegar, J.; Pereira, C.; Nguyen, H.L. Piezoelectric-based power sources for harvesting energy from platforms with low-frequency vibration. In Proceedings of the Smart Structures and Materials 2006: Industrial and Commercial Applications of Smart Structures Technologies, San Diego, CA, USA, 27–28 February 2006; Volume 6171. [[CrossRef](#)]
10. Renaud, M.; Fiorini, P.; van Schaijk, R.; van Hoof, C. Harvesting energy from the motion of human limbs: The design and analysis of an impact-based piezoelectric generator. *Smart Mater. Struct.* **2009**, *18*, 035001. [[CrossRef](#)]
11. Gu, L.; Livermore, C. Impact-driven, frequency up-converting coupled vibration energy harvesting device for low frequency operation. *Smart Mater. Struct.* **2011**, *20*, 045004. [[CrossRef](#)]
12. Halim, M.A.; Park, J.Y. Theoretical modeling and analysis of mechanical impact driven and frequency up-converted piezoelectric energy harvester for low-frequency and wide-bandwidth operation. *Sens. Actuators A Phys.* **2014**, *208*, 56–65. [[CrossRef](#)]
13. Zhang, Y.; Cai, C.S. A retrofitted energy harvester for low frequency vibrations. *Smart Mater. Struct.* **2012**, *21*, 075007. [[CrossRef](#)]
14. Wei, S.; Hu, H.; He, S. Modeling and experimental investigation of an impact-driven piezoelectric energy harvester from human motion. *Smart Mater. Struct.* **2013**, *22*, 105020. [[CrossRef](#)]
15. Pozzi, M.; Zhu, M. Plucked piezoelectric bimorphs for knee-joint energy harvesting: Modelling and experimental validation. *Smart Mater. Struct.* **2011**, *20*, 055007. [[CrossRef](#)]
16. Liu, T.; Pierre, R.S.; Livermore, C. Passively-switched energy harvester for increased operational range. *Smart Mater. Struct.* **2014**, *23*, 095045. [[CrossRef](#)]
17. Chen, S.; Ma, L.; Chen, T.; Liu, H.; Sun, L.; Wang, J. Modeling and verification of a piezoelectric frequency-up-conversion energy harvesting system. *Microsyst. Technol.* **2016**. [[CrossRef](#)]
18. Vijayan, K.; Friswell, M.I.; Haddad Khodaparast, H.; Adhikari, S. Non-linear energy harvesting from coupled impacting beams. *Int. J. Mech. Sci.* **2015**, *96–97*, 101–109. [[CrossRef](#)]
19. Edwards, B.; Hu, P.A.; Aw, K.C. Validation of a hybrid electromagnetic–piezoelectric vibration energy harvester. *Smart Mater. Struct.* **2016**, *25*, 055019. [[CrossRef](#)]
20. Xu, Z.; Shan, X.; Chen, D.; Xie, T. A Novel Tunable Multi-Frequency Hybrid Vibration Energy Harvester Using Piezoelectric and Electromagnetic Conversion Mechanisms. *Appl. Sci. (Basel)* **2016**, *6*, 10. [[CrossRef](#)]
21. Xu, Z.; Shan, X.; Yang, H.; Wang, W.; Xie, T. Parametric Analysis and Experimental Verification of a Hybrid Vibration Energy Harvester Combining Piezoelectric and Electromagnetic Mechanisms. *Micromachines (Basel)* **2017**, *8*, 189. [[CrossRef](#)]
22. Tang, L.; Yang, Y. A nonlinear piezoelectric energy harvester with magnetic oscillator. *Appl. Phys. Lett.* **2012**, *101*, 094102. [[CrossRef](#)]
23. Stephen, N.G. On energy harvesting from ambient vibration. *J. Sound Vib.* **2006**, *293*, 409–425. [[CrossRef](#)]
24. Qi, X.; Yin, X. Experimental studying multi-impact phenomena exhibited during the collision of a sphere onto a steel beam. *Adv. Mech. Eng.* **2016**, *8*, 1–16. [[CrossRef](#)]
25. Stanton, S.C.; Erturk, A.; Mann, B.P.; Dowell, E.H.; Inman, D.J. Nonlinear nonconservative behavior and modeling of piezoelectric energy harvesters including proof mass effects. *J. Intell. Mater. Syst. Struct.* **2012**, *23*, 183–199. [[CrossRef](#)]



© 2017 by the authors. Licensee MDPI, Basel, Switzerland. This article is an open access article distributed under the terms and conditions of the Creative Commons Attribution (CC BY) license (<http://creativecommons.org/licenses/by/4.0/>).